Manuscript Title:

Meta-analysis of apparent diffusion coefficient in pediatric medulloblastoma, ependymoma and pilocytic astrocytoma

Abstract:

Background: Medulloblastoma, ependymoma and pilocytic astrocytoma are common pediatric posterior fossa tumors. These tumors show overlapping characteristics on conventional MRI scans, making diagnosis difficult.

Purpose: To investigate whether apparent diffusion coefficient (ADC) values differ between tumor types, and to identify optimum cut-off values to accurately classify the tumors using different performance metrics.

Study type: Systematic review and meta-analysis.

Subjects: 7 studies reporting ADC in pediatric posterior fossa tumors (115 medulloblastoma, 68 ependymoma and 86 pilocytic astrocytoma) were included following PubMed and ScienceDirect searches.

Sequence and field strength: Diffusion weighted imaging (DWI) was performed on 1.5 and 3T across multiple institution and vendors.

Assessment: The combined mean and standard deviation of ADC were calculated for each tumor type using a random-effects model, and the effect size was calculated using Hedge's g.

Statistical tests: Sensitivity/specificity, weighted classification accuracy, balanced classification accuracy. A p value < 0.05 was considered statistically significant, and a Hedge's g value of >1.2 was considered to represent a large difference.

Results: The mean (± standard deviation) ADCs of medulloblastoma, ependymoma and pilocytic astrocytoma were 0.76 ± 0.16, 1.10 ± 0.10 and 1.49 ± 0.16 mm^2/s $x10^{-3}$. To maximize sensitivity and specificity using the mean ADC, the cut-off was found to be 0.96 mm^2/s $x10^{-3}$ for medulloblastoma and ependymoma and 1.26 mm^2/s $x10^{-3}$ for ependymoma and pilocytic astrocytoma. The meta-analysis showed significantly different ADC distributions for the three posterior fossa tumors. The cut-off values changed markedly (up to 7%) based of the performance metric used and the prevalence of the tumor types.

Data conclusion: There were significant differences in ADC between tumor types. However, it should be noted that only summary statistics from each study were analyzed and there were differences in how regions of interest were defined between studies.

Keywords (6):

ADC, Meta-Analysis, Medulloblastoma, Ependymoma, Pilocytic Astrocytoma, Pediatric.

Introduction

Posterior fossa tumors account for around 60% of pediatric brain tumors [1]. The three most common pediatric posterior fossa tumor types are medulloblastoma, ependymoma and pilocytic astrocytoma [2]. There are important differences in the incidence, malignancy, frequency of metastases and outcome for these tumors [2-5], as well as different therapeutic strategies based on tumor type and histological subtypes.

Ependymoma which is a very 'surgical' tumor has a prognosis which is heavily dependent on completeness of resection [6]. Conversely in Pilocytic astrocytoma which can sometimes be a very infiltrative entity, tumor may be intentionally left behind due to its location and anticipated relatively benign course [7]. Similarly, tumors suspected of being medulloblastomas may be intentionally sub-totally resected due to concerns of a high risk of causing a posterior fossa syndrome by aggressively chasing invasive tumor in the cerebellar peduncles when that tumor may subsequently be very responsive to adjuvant post-operative therapies[8]. The surgical strategy does then vary considerably between these three commonest entities, and it would be extremely useful for surgeons to have a reliable indication of diagnosis while they are planning and carrying out surgery.

Unfortunately, however, diagnosis of posterior fossa tumor type can be difficult prior to surgery, with significant overlap in imaging characteristics between tumor types on conventional MRI [9]. Tissue taken during biopsy or surgical resection provides the diagnostic 'reference standard', ultimately allowing histological and molecular characterization of the tumor. During surgery a smear preparation may be quickly carried out on a specimen and phoned back to theatre within 30 minutes, but it is difficult for neuropathologists to give a very confident smear diagnosis in many cases,

and it can be difficult to distinguish ependymoma from medulloblastoma on smear with both appearing as small blue cell tumors. In retrospective review of operation notes during the analysis of a multi-center ependymoma study by one of the authors (DCM) the smear diagnosis was either uncertain or actively misleading in over 50% of cases so there is a clear opportunity to improve on this by considering any additional available pre-operative information.

Diffusion weighted imaging (DWI) is a quantitative MRI technique that provides spatial information on the random motion of water molecules in tissue, combining intra-, trans-, and extra-cellular diffusion as well as perfusion[10]. The apparent diffusion coefficient (ADC) is a quantitative value that can be obtained from DWI and describes the magnitude of the motion of water molecules independent of direction [11]. A meta-analysis performed by *Surov et al.* [12] demonstrated a strong inverse relationship between ADC and the density of tumorous tissue cells. There are known differences in the cellularity of medulloblastoma, ependymoma and pilocytic astrocytoma[13] which makes DWI a promising method to distinguish tumor types.

The profile of ADC in pediatric posterior fossa tumors has been widely investigated [13-30]. It is broadly recognized in clinical practice that medulloblastoma typically show reduced ADC within the tumor compared to surrounding tissues, pilocytic astrocytoma typically show elevated ADC compared to surrounding tissue, and that ependymomas typically 'sit in the middle', often demonstrating mixed ADC values including areas of low and high ADC[30]. Many studies in the literature consider the mean ADC within the tumor region-of-interest (ROI) and use this value to identify differences between tumor types [14-18, 20-23, 25-29, 31, 32], and to identify the optimal cut-offs for distinguishing tumor types [18-24, 26, 28, 29]. In addition, histogram analyses have been performed to identify percentiles that distinguish tumor types [15, 22, 23, 25, 28]. While these previous studies have

demonstrated that ADC has the potential to be a useful marker for differentiating tumor types, there are currently no consensus values. Thus the aim of this study was to perform a meta-analysis of previous studies reporting the mean ADC within either pediatric medulloblastoma, ependymoma or pilocytic astrocytoma and to:

1. Establish the mean ADC values for different tumor types.
2. Calculate the effect sizes between the different tumor types
3. Establish the optimum cut-off or threshold values of mean ADC for differentiating the tumor types using sensitivity/specificity, weighted and balanced classification accuracy.

We hope that the results presented here will serve as an aid to the existing methods of the differential diagnosis of medulloblastoma, ependymoma and pilocytic astrocytoma to give more confidence towards earlier diagnosis.

Methods

Systematic Review

The meta-analysis had no documented protocol. However, the preferred reporting items for systematic reviews and meta-analyses (PRISMA) guidelines were used for reporting [33].

A systematic review of published literature was conducted to establish the performance characteristics of DWI for differentiating pediatric posterior fossa tumor types as detailed above. For inclusion, studies needed to report the mean ADC value derived from DWI performed prior to surgery of either medulloblastoma, ependymoma or pilocytic astrocytoma. Only studies which contained pediatric cohorts (participants <21 years) with a subsequent histological diagnosis were included. This required the age range to be explicitly stated and not summarized as a mean and standard deviation.

Studies were also required to have described the method for defining the region-of-interest (ROI) for ADC calculation in terms of the included tumor components (solid only, solid, and cystic, etc). Subsequently, only papers which extracted the ADC from solid portions of the tumor and excluded necrotic, cystic and hemorrhagic regions were included in the analysis. Studies were also required to have reported the ADC in absolute units of mm^2/s, or if the relative ADC was reported, the scaling factor must have been provided. The systematic review was of the pre-surgery diagnostic imaging and there were no restrictions to the inclusion of studies based on subsequent interventions. At least 5 samples for each tumor type were required in order for a study to be included. Studies collecting data from both 1.5T and 3T scanners were included with no restriction on vendor.

Studies were identified by searching electronic databases and scanning reference lists of articles. No restrictions were placed on the language used to report the study. This search was applied to PubMed and ScienceDirect with no restrictions on publication date. Combinations of the following search terms were used to search the databases: medulloblastoma; ependymoma; pilocytic astrocytoma; posterior fossa; ADC; apparent diffusion coefficient (**Appendix 1**).

Data were extracted from published articles for each tumor type regarding number of tumors included in the analysis, mean ADC and standard deviation. If the individual data points were not reported for each patient, the reported ADC and standard deviation over all patients was used. Additionally, if data were only available through figures or graphs, the data points were determined directly from the figures.

Risk of bias across the studies was assessed using the I^2 value calculated for differences between independent groups. Heterogeneity calculations were performed

using the Meta-Essentials tool [34]. Additionally, the QUADAS-2 bias assessment tool [35] was used to understand the risk of bias.

Meta-Analysis

For each tumor type, a combined mean and standard deviation were calculated for mean ADC using a random-effects model. A Shapiro-Wilks test [36] was performed to ensure that the combined distributions across different studies could be treated as Gaussian. The distributions of ADC values for each tumor were therefore treated as perfect Gaussians defined by the combined mean and standard deviation obtained using the random-effects model. To account for the prevalence of these tumors, the probability distribution function for each tumor was multiplied by their prevalence. They were then normalized to the area under the distribution of the tumors of interest.

The effect sizes between the tumors was calculated according the Hedge's g using the Meta-Essentials tool [34]. To assess the magnitude of this effect size, the method described in Sawilowsky et al., [37] was used.

In this meta-analysis, three cut-offs were calculated: the cut-off between medulloblastoma and ependymoma (α), ependymoma and pilocytic astrocytoma (β) and medulloblastoma and pilocytic astrocytoma (γ). The optimization of these cut-offs was calculated by either including all three tumors simultaneously, or by just using any two tumors of interest. Including all three tumors simultaneously maximized the performance if all three tumor types were candidates. However, if the observer could be confident of excluding one of the tumors as a candidate, then the more simplified analysis was used. The cut-offs were optimized for mean ADC using multiple performance metrics; sensitivity and specificity, and weighted and balanced

classification accuracy. Additionally, the prevalence of each tumor type in a pediatric cohort [2] was considered in the calculation.

Statistical Analysis

The performance metrics used to optimize the cut-offs required the true positive (TP), false positive (FP), true negative (TN) and false negative (FN) statistics to be calculated. The equation for these when considering two tumors followed standard methodology, however some modifications were made when considering all three groups (**Table 1**). Using these, the standard definitions for sensitivity and specificity, weighted and balanced classification accuracy were calculated for each tumor type.

TP, TN, FP, FN were calculated analytically by using the Gaussian cumulative distribution function (CDF) between cut-offs and multiplying by the tumor's prevalence. To determine the optimum cut-offs, the sum of square differences between the measured performance and its maximum score were minimized.

In order for the combined summary results to be considered normally distributed, a p-value of <0.05 must be calculated using the Shaprio-Wilks test.

The coefficient of variation for the ADC of each tumor type is calculated by dividing the standard deviation by the mean (σ/μ).

Results

A total of 1404 unique studies were identified using the search strategy described. The study titles were screened for relevance which reduced the number to 31 papers. Twenty four were discarded after a full text review as they did not meet the inclusion criteria. Seven papers were ultimately identified which reported mean ADC while

matching the inclusion criteria [16, 21, 27, 29-32] (**Figure 1**). Only one of these studies collected data from multiple scanners across multiple institutions [30].

Six of the seven studies acquired DWI echo planar imaging (EPI) acquisitions [21, 27, 29-32]. Of these 6 studies, repetition times ranged from 2435 to 8575 ms, echo times ranged from 60-161 ms, slices thickness ranged from 4 to 6 mm and slice gaps ranged from 0 to 3 mm. These 6 studies acquired b-values of 0 and 1000, with one study also acquiring an additional b-value of 500 [27]. One study in the final cohort did not report any DWI parameters [16]. Three studies acquired data solely from Philips Achieva 1.5T scanners [16, 21, 32], one study acquired data solely from a Siemens 1.5T scanner [27], one study acquired data solely from a GE 1.5 T scanner and two studies combined data from multiple scanners [29, 30]. Only one study included the use of 3T MRI scanners [30], and was also the only multi-institutional study (**Table 2**).

When assessing the bias across studies using I^2 between tumor types, heterogeneity was found to be negligible for medulloblastoma/pilocytic astrocytoma and ependymoma/pilocytic astrocytoma (<25%). However, medulloblastoma / ependymoma heterogeneity was calculated to be 53.4% which suggested moderate heterogeneity.

When assessing bias using the QUADAS-2 tool, we found that most of the studies (5/7) presented low bias and no applicability concerns. However, we found that the reference standard used in two studies [21, 32] presented high bias as CT imaging was preferred for diagnosis over gold-standard histology reports (**Appendix 2**).

Studies reporting the mean ADC included 115 medulloblastoma, 68 ependymoma and 86 pilocytic astrocytoma. It was found that medulloblastoma had a mean (± standard deviation) ADC of 0.76 ± 0.16 mm^2 /s $x10^{-3}$, ependymoma had a mean ADC of 1.10 ±

0.10 mm^2 /s $x10^{-3}$ and pilocytic astrocytoma had a mean ADC of 1.49 ± 0.16 mm^2 /s $x10^{-3}$ (**Table 3**,**Table 4** and **Figure 2**). The combined data from the literature demonstrated normality, with mean ADC values for all tumors passing the Shapiro-Wilks test.

The effect size between medulloblastoma and ependymoma was 3.19 for mean ADC. For medulloblastoma and pilocytic astrocytoma, the effect size was 3.43, and for ependymoma and pilocytic astrocytoma the effect size was 1.81.

The optimized cut-offs and performance metrics between tumor types for mean ADC are reported in **Table 5**. The inclusion of all three tumors using the modified equations shown in **Table 1** had a minor effect on the cut-offs compared to the two group case (**Appendix 3**). The choice of metric had a large effect on cut-offs, with both weighted and balanced classification accuracy increasing $\propto$ and decreasing β, thus narrowing the window for ependymoma. Typically, medulloblastoma and pilocytic astrocytoma had the best performance when all three tumor types were included in the optimization algorithm. However, the performance metrics for the cut-offs ependymoma improved when compared to just one other tumor type.

Discussion

We employed standardized systematic review methodology and performed a quantitative synthesis of the literature which confirmed that mean ADC values differ between the three most common pediatric posterior fossa tumor types, being lowest in medulloblastoma, highest in pilocytic astrocytoma and intermediate in ependymoma. We calculated effect sizes, and cut-off values optimized for overall sensitivity and specificity, and for weighted and balanced classification accuracy.

The meta-analysis ultimately identified 7 studies reporting the mean ADC. The effect size for mean ADC was large between all tumor types, suggesting that the observed differences between the tumor types were significant [37]. The mean ADC for ependymoma was between the means of medulloblastoma and pilocytic astrocytoma, and these are the hardest to separate. However, the large effect size between the other tumor types suggests that with a large enough sample size, ependymoma possesses a significantly different mean ADC to the other two tumor types. This reinforces the results from most of the previous literature that state that ependymoma has a significantly higher ADC than medulloblastoma, but significantly lower than pilocytic astrocytoma[29, 30]. In this study, the effect size between medulloblastoma and pilocytic astrocytoma was large, and represented a “huge” [37]. These results suggest that between all tumor types there is a significant difference in the mean ADC.

The overlap of distributions (particularly from ependymoma) poses a challenge for clinical diagnosis of individual cases. To assess the diagnostic performance of mean ADC, we optimized cut-offs between tumor types to maximize sensitivity/specificity, and weighted and balanced classification accuracy. Each performance metric measures the diagnostic potential differently; sensitivity/specificity and balanced classification accuracy ensure that less prevalent tumors are weighted equally to other more prominent tumors. However, the balanced classification accuracy is only concerned with the number of true positives from each group and ignores the number of false positives from other groups. Weighted classification accuracy is also only concerned with true positives, but additionally considers the prevalence of the tumors so the most common tumor strongly influences the optimization. The metric to be used is dependent on the problem one is trying to solve. If achieving the highest overall accuracy of diagnosis is the aim, then the weighted or balanced classification accuracy

would be appropriate. However, if maximizing the chance of correctly diagnosing each individual case is the aim, then sensitivity/specificity would be best suited.

While we have included an assessment of the diagnostic accuracy when two tumors are considered, a scenario when this is appropriate is rare. The study rationale presents the issue that an observer would not which of the three tumors on is dealing with, and therefore a tumor type cannot be excluded from the assessment.

The performance metrics drive the calculated optimum cut-offs. When sensitivity and specificity are considered, the cut-off between medulloblastoma and ependymoma is lower than when using weighted classification accuracy. Additionally, the cut-off between ependymoma and pilocytic astrocytoma decreases when using weighted classification accuracy over sensitivity/specificity. This is expected as optimizing based on classification accuracy is equivalent to maximizing the number of true positives, which means that more emphasis is put on correctly classifying the most prevalent tumors. As ependymoma is least prevalent (15% of all posterior fossa tumors [2]) and its ADC sits between two more common tumors, it follows that the range between the cut-offs narrows.

Some of the studies included have also reported optimal cut-offs between tumors for mean ADC [21, 24, 30]. When considering the cut-off between medulloblastoma and ependymoma, values from 0.90 to 0.98 mm^2/s $x10^{-3}$ have been reported [21, 24, 30]. This range is similar to that predicted in this meta-analysis when using the sensitivity/specificity performance metric. For ependymoma and pilocytic astrocytoma, a value of 1.30 mm^2/s $x10^{-3}$ was presented in the literature[21] which is similar to that calculated using balanced classification accuracy in this study. These similarities

increase confidence that the cut-offs derived in this meta-analysis can be applied to other samples.

The definition of the ROI used to calculate the mean ADC was part of the eligibility criteria for this study, in order to ensure that the results between included studies were as comparable as possible. Necrotic and cystic components of tumors are known to have very high ADC values compared to the tumor tissue, so the inclusion of these regions would artificially increase the measured ADC of the tumor[38]. Studies which included large areas of these components were therefore excluded during study selection. Despite these criteria being applied, it must be stated that the ROIs of the included studies do have distinct differences. Four of the 7 included studies explicitly stated that only solid portions of the tumor were considered and necrotic, cystic and hemorrhagic regions were excluded [16, 29-31]. Two further studies defined their ROIs as the enhancing portion of the tumor [21, 32]and these were included as only solid tumor tissue enhances. Finally, *one study* [27] placed a single ROI inside the solid and non-necrotic area of the tumor. Despite this not capturing the extent of the tumor tissue, what was included was solid tumor tissue and this study was therefore deemed eligible (**Table 2**).

Care was taken to ensure that the data extracted from all studies was in the same form, however some approximations had to be made to achieve this. Some studies reported data in the form of a median and range [14, 17, 18, 27], which could be transformed into a mean and standard deviation [39]. This may lead to slightly biased estimates depending on the true shape of the distribution; however, these studies were still included to maximize the number of samples. Additionally, some data points were also calculated directly from figures [19] which will also possess some error, however it was decided that the benefit of increased sample size was worth this.

As well as mean ADC, minimum ADC is sometimes used in order to identify these posterior fossa tumors. However, during the systematic search and subsequently applying the inclusion criteria, only two studies were eligible. We felt that two studies did not yet warrant a meta-analysis, and that the results obtained would not possess sufficient power to be compared to the mean ADC.

In clinical practice, mean ADC values are not used in isolation; other imaging features (such as tumor morphology or spectroscopy) or clinical parameters are taken into account during the diagnostic radiological process. However, we believe that the results presented can aid current differential diagnosis of pediatric medulloblastoma, ependymoma and pilocytic astrocytoma by providing rigorously assessed cutoff values for mean ADC with different performance metrics.

Mean ADC values assessed ahead of surgery, and especially when considering other imaging features as well as information from intraoperative smears, could potentially greatly increase the degree of diagnostic certainty that surgeons have during posterior fossa tumor resections and in turn influence their surgical strategy in carrying out the optimal resection for that particular patient.

Limitations

This study suffered from some unavoidable limitations, with one being the small number of studies included in the meta-analysis. Care was taken to ensure that the studies selected were as homogenous as possible, which was achieved with a strict eligibility criterion. This had the consequence of returning a relatively small number of eligible studies for a meta-analysis, and hence a small number of samples. Ideally a larger number of studies would have been desired, however, we believe that this

criterion has provided the most accurate analysis of ADC of pediatric posterior fossa tumors.

Despite the eligibility criteria ensuring that the ROI used to measure mean ADC only included solid tumor tissue, the included studies demonstrated variability in ROI definition. This may have an impact on the reported ADC values from each of the study and in turn affect this meta-analysis.

A final limitation was the retrieval of ADC measures from the listed studies. The desired metric was mean ADC, however some papers did not explicitly report this and had to be calculated from figures or converted from other summary metrics. Therefore, the true, unreported means from these studies are estimated here using accepted methods.

In this study we have represented the ADC distribution from each tumor type as an idealized Gaussian. As such, the optimization calculations for the cut-offs and the diagnostic accuracies are based on simulated data. In order for these cut-offs to be validation an Independent Patient Data meta-analysis or consecutive cohort of patients is required.**Conclusions**

This meta-analysis provides mean ADC values for the three most common types of pediatric posterior fossa tumor types. Cut-off values for mean ADC values for distinguishing tumor types have been calculated based on maximizing sensitivity and specificity and weighted and balanced classification accuracy. Our work provides a quantitative basis for tumor classification based on ADC values that may aid the diagnostic process or have value in further posterior fossa tumor research.

Funding

Funding for this project was provided by Children with Cancer (CwC) and the Children's Cancer and Leukemia Group (CCLG).

References

1. O'Brien DF, Caird J, Kennedy M, Roberts GA, Marks JC, Allcutt DA. Posterior fossa tumours in childhood: evaluation of presenting clinical features. *Ir Med J*. Feb 2001;94(2):52-3.

2. Stiller CA, Bayne AM, Chakrabarty A, Kenny T, Chumas P. Incidence of childhood CNS tumours in Britain and variation in rates by definition of malignant behaviour: population-based study. *BMC Cancer*. Feb 11 2019;19(1):139. doi:10.1186/s12885-019-5344-7

3. Dufour C, Beaugrand A, Pizer B, et al. Metastatic Medulloblastoma in Childhood: Chang's Classification Revisited. *Int J Surg Oncol*. 2012;2012:245385. doi:10.1155/2012/245385

4. Benesch M, Mynarek M, Witt H, et al. Newly Diagnosed Metastatic Intracranial Ependymoma in Children: Frequency, Molecular Characteristics, Treatment, and Outcome in the Prospective HIT Series. *Oncologist*. Sep 2019;24(9):e921-e929. doi:10.1634/theoncologist.2018-0489

5. Peyre M, Commo F, Dantas-Barbosa C, et al. Portrait of ependymoma recurrence in children: biomarkers of tumor progression identified by dual-color microarray-based gene expression analysis. *PLoS One*. Sep 24 2010;5(9):e12932. doi:10.1371/journal.pone.0012932

6. Ruda R, Reifenberger G, Frappaz D, et al. EANO guidelines for the diagnosis and treatment of ependymal tumors. *Neuro Oncol*. Mar 27 2018;20(4):445-456. doi:10.1093/neuonc/nox166

7. Villanueva KG, Rea ND, Krieger MD. Novel Surgical and Radiologic Risk Factors for Progression or Recurrence of Pediatric Pilocytic Astrocytoma. *Pediatr Neurosurg*. 2019;54(6):375-385. doi:10.1159/000503110

8. Pols S, van Veelen MLC, Aarsen FK, Gonzalez Candel A, Catsman-Berrevoets CE. Risk factors for development of postoperative cerebellar mutism syndrome in children after medulloblastoma surgery. *J Neurosurg Pediatr*. Jul 2017;20(1):35-41. doi:10.3171/2017.2.PEDS16605

9. Dong J, Li L, Liang S, et al. Differentiation Between Ependymoma and Medulloblastoma in Children with Radiomics Approach. *Acad Radiol*. Mar 25 2020;doi:10.1016/j.acra.2020.02.012

10. Hagmann P, Jonasson L, Maeder P, Thiran JP, Wedeen VJ, Meuli R. Understanding diffusion MR imaging techniques: from scalar diffusion-weighted imaging to diffusion tensor imaging and beyond. *Radiographics*. Oct 2006;26 Suppl 1:S205-23. doi:10.1148/rg.26si065510

11. Baliyan V, Das CJ, Sharma R, Gupta AK. Diffusion weighted imaging: Technique and applications. *World J Radiol*. Sep 28 2016;8(9):785-798. doi:10.4329/wjr.v8.i9.785

12. Surov A, Meyer HJ, Wienke A. Correlation between apparent diffusion coefficient (ADC) and cellularity is different in several tumors: a meta-analysis. *Oncotarget*. Aug 29 2017;8(35):59492-59499. doi:10.18632/oncotarget.17752

13. Yamashita Y, Kumabe T, Higano S, Watanabe M, Tominaga T. Minimum apparent diffusion coefficient is significantly correlated with cellularity in

medulloblastomas. *Neurol Res*. Nov 2009;31(9):940-6. doi:10.1179/174313209X382520

14. Assis ZA, Saini J, Ranjan M, Gupta AK, Sabharwal P, Naidu PR. Diffusion tensor imaging in evaluation of posterior fossa tumors in children on a 3T MRI scanner. *Indian J Radiol Imaging*. Oct-Dec 2015;25(4):445-52. doi:10.4103/0971-3026.169444

15. Bull JG, Saunders DE, Clark CA. Discrimination of paediatric brain tumours using apparent diffusion coefficient histograms. *Eur Radiol*. Feb 2012;22(2):447-57. doi:10.1007/s00330-011-2255-7

16. Dominguez-Pinilla N, Martinez de Aragon A, Dieguez Tapias S, et al. Evaluating the apparent diffusion coefficient in MRI studies as a means of determining paediatric brain tumour stages. *Neurologia*. Sep 2016;31(7):459-65. Evaluacion de la utilidad del coeficiente de difusion aparente en resonancia magnetica para la diferenciacion del grado tumoral de los tumores cerebrales pediatricos. doi:10.1016/j.nrl.2014.12.003

17. Gauvain KM, McKinstry RC, Mukherjee P, et al. Evaluating pediatric brain tumor cellularity with diffusion-tensor imaging. *AJR Am J Roentgenol*. Aug 2001;177(2):449-54. doi:10.2214/ajr.177.2.1770449

18. Gimi B, Cederberg K, Derinkuyu B, et al. Utility of apparent diffusion coefficient ratios in distinguishing common pediatric cerebellar tumors. *Acad Radiol*. Jul 2012;19(7):794-800. doi:10.1016/j.acra.2012.03.004

19. Jaremko JL, Jans LB, Coleman LT, Ditchfield MR. Value and limitations of diffusion-weighted imaging in grading and diagnosis of pediatric posterior fossa tumors. *AJNR Am J Neuroradiol*. Oct 2010;31(9):1613-6. doi:10.3174/ajnr.A2155

20. Koral K, Alford R, Choudhury N, et al. Applicability of apparent diffusion coefficient ratios in preoperative diagnosis of common pediatric cerebellar tumors across two institutions. *Neuroradiology*. Sep 2014;56(9):781-8. doi:10.1007/s00234-014-1398-z

21. Mohamed FF, Azeem Ismail AA, Hasan DI, Essa WE. The role of apparent diffusion coefficient (ADC) value in the differentiation between the most common pediatric posterior fossa tumors. *The Egyptian Journal of Radiology and Nuclear Medicine*. 2013/06/01/ 2013;44(2):349-355. doi:https://doi.org/10.1016/j.ejrnm.2012.12.011

22. Payabvash S, Tihan T, Cha S. Volumetric voxelwise apparent diffusion coefficient histogram analysis for differentiation of the fourth ventricular tumors. *Neuroradiol J*. Dec 2018;31(6):554-564. doi:10.1177/1971400918800803

23. Payabvash S, Tihan T, Cha S. Differentiation of Cerebellar Hemisphere Tumors: Combining Apparent Diffusion Coefficient Histogram Analysis and Structural MRI Features. *J Neuroimaging*. Nov 2018;28(6):656-665. doi:10.1111/jon.12550

24. Pierce T, Kranz PG, Roth C, Leong D, Wei P, Provenzale JM. Use of apparent diffusion coefficient values for diagnosis of pediatric posterior fossa tumors. *Neuroradiol J*. Apr 2014;27(2):233-44. doi:10.15274/NRJ-2014-10027

25. Rodriguez Gutierrez D, Awwad A, Meijer L, et al. Metrics and textural features of MRI diffusion to improve classification of pediatric posterior fossa tumors. *AJNR Am J Neuroradiol*. May 2014;35(5):1009-15. doi:10.3174/ajnr.A3784

26. Rumboldt Z, Camacho DL, Lake D, Welsh CT, Castillo M. Apparent diffusion coefficients for differentiation of cerebellar tumors in children. *AJNR Am J Neuroradiol*. Jun-Jul 2006;27(6):1362-9.

27. Schneider JF, Confort-Gouny S, Viola A, et al. Multiparametric differentiation of posterior fossa tumors in children using diffusion-weighted imaging and short echo-time 1H-MR spectroscopy. *J Magn Reson Imaging*. Dec 2007;26(6):1390-8. doi:10.1002/jmri.21185

28. Wang W, Cheng J, Zhang Y, Wang C. Use of Apparent Diffusion Coefficient Histogram in Differentiating Between Medulloblastoma and Pilocytic Astrocytoma in Children. *Med Sci Monit*. Sep 2 2018;24:6107-6112. doi:10.12659/MSM.909136

29. Zitouni S, Koc G, Doganay S, et al. Apparent diffusion coefficient in differentiation of pediatric posterior fossa tumors. *Jpn J Radiol*. Aug 2017;35(8):448-453. doi:10.1007/s11604-017-0652-9

30. Novak J, Zarinabad N, Rose H, et al. Classification of paediatric brain tumours by diffusion weighted imaging and machine learning. *Sci Rep*. Feb 4 2021;11(1):2987. doi:10.1038/s41598-021-82214-3

31. Chen HJ, Panigrahy A, Dhall G, Finlay JL, Nelson MD, Jr., Bluml S. Apparent diffusion and fractional anisotropy of diffuse intrinsic brain stem gliomas. *AJNR Am J Neuroradiol*. Nov 2010;31(10):1879-85. doi:10.3174/ajnr.A2179

32. Taheri H, Tavakoli MB. Measurement of Apparent Diffusion Coefficient (ADC) Values of Ependymoma and Medulloblastoma Tumors: a Patient-based Study. *J Biomed Phys Eng*. Feb 2021;11(1):39-46. doi:10.31661/jbpe.v0i0.889

33. Moher D, Liberati A, Tetzlaff J, Altman DG, Group P. Preferred reporting items for systematic reviews and meta-analyses: the PRISMA statement. *PLoS Med*. Jul 21 2009;6(7):e1000097. doi:10.1371/journal.pmed.1000097

34. Suurmond R, van Rhee H, Hak T. Introduction, comparison, and validation of Meta-Essentials: A free and simple tool for meta-analysis. *Res Synth Methods*. Dec 2017;8(4):537-553. doi:10.1002/jrsm.1260

35. Whiting PF, Rutjes AW, Westwood ME, et al. QUADAS-2: a revised tool for the quality assessment of diagnostic accuracy studies. *Ann Intern Med*. Oct 18 2011;155(8):529-36. doi:10.7326/0003-4819-155-8-201110180-00009

36. Shapiro SS, Wilk MB. An Analysis of Variance Test for Normality (Complete Samples). *Biometrika*. 1965;52(3/4):591-611. doi:10.2307/2333709

37. Sawilowsky S. New Effect Size Rules of Thumb. *Journal of Modern Applied Statistical Methods*. 11/01 2009;8:597-599. doi:10.22237/jmasm/1257035100

38. Pekcevik Y, Kahya MO, Kaya A. Characterization of Soft Tissue Tumors by Diffusion-Weighted Imaging. *Iran J Radiol*. Jul 2015;12(3):e15478. doi:10.5812/iranjradiol.15478v2

39. Hozo SP, Djulbegovic B, Hozo I. Estimating the mean and variance from the median, range, and the size of a sample. *BMC Med Res Methodol*. Apr 20 2005;5:13. doi:10.1186/1471-2288-5-13

Tables

	Medulloblastoma	**Ependymoma**	**Pilocytic Astrocytoma**
True Positive (TP)	$\mathrm{MB}_N \leq \alpha$	$\mathrm{EP}_N > \alpha \cap \mathrm{EP}_N \leq \beta$	$\mathrm{PA}_N > \beta$
True Negative (TN)	$\mathrm{EP}_N > \alpha + \mathrm{PA}_N > \alpha$	$\mathrm{MB}_N \leq \alpha + \mathrm{PA}_N > \beta$	$\mathrm{MB}_N \leq \beta + \mathrm{EP}_N \leq \beta$
False Positive (FP)	$\mathrm{EP}_N \leq \alpha + \mathrm{PA}_N \leq \alpha$	$\mathrm{MB}_N > \alpha + \mathrm{PA}_N \leq \beta$	$\mathrm{MB}_N > \beta + \mathrm{EP}_N > \beta$
False Negative (FN)	$\mathrm{MB}_N > \alpha$	$\mathrm{EP}_N \leq \alpha \cup \mathrm{EP}_N > \beta$	$\mathrm{PA}_N \leq \beta$

Table 1 *- Table showing the modified conditions for calculating the number of True Positives, True Negatives, False Positives and False Negatives when all three tumors are candidates.* MB_N, EP_N *and* PA_N *represent the number of medulloblastoma, ependymoma and pilocytic astrocytoma.*

Study	MRI Scanner	Repetition Time (ms)	Echo Time (ms)	Slice Thickness (mm)	Slice Gap (mm)	FOV (mm)	b-Values	ROI Definition	Reference Standard
Domínguez-Pinilla (2016)*	Philips 1.5T	-	-	-	-	-	0-1000	“in the solid portion of the tumor, excluding possibly artifacted areas”	WHO Histology
Mohamed (2013)	Philips 1.5T	4200	140	5	0	240x240	0-1000	“enhancing solid portion of the lesion after it was identified on post contrast axial, coronal and sagittal T1 WIs and in the normal brain tissue”	CT diagnosis
Schneider (2007)	Siemens 1.5T	3600	107	5	0	240x240	0-1000	“A single-sized region of interest (ROI) of 43.3 mm2 was placed within the solid and nonnecrotic area of tumorous tissue”	WHO Histology
Zitouni (2017)	Philips/Siemens 1.5T	3500	83	5	0.5	230x230	0-1000	“Region of interest measurements were obtained from the solid component of the tumoral lesions with the lowest signal on ADC maps, excluding necrotic and hemorrhagic areas”	WHO Histology
Novak (2021)	Philips/Siemens/GE 1.5/3T	2435-8575	60-161	4-6	0.4-3	163	0-1000	“Regions of interest were drawn manually for the whole tumors excluding areas of large cysts and peri-tumoral oedema using MRIcron”	WHO Histology
Taheri (2021)	Philips 1.5T	4400	110	5	1	240x240	0-1000	“The enhancing solid portion of stated lesions was identified on post-contrast T1 W images and the matching ADC maps for each patient. Regions of	CT diagnosis

								interest (ROIs) were drawn in the ADC maps”	
Chen (2010)	GE 1.5T	-	85	5-7	0	200-260	0-1000	“Areas with necrosis and cystic degeneration were excluded to the extent possible”	WHO Histology

Table 2 *– Summary of DWI acquisition parameters and ROI definitions of the seven studies included in the meta-analysis.* Study did not report DWI acquisition parameters.*

	Mean ADC ± Standard Deviation (mm^2 / s $x10^{-3}$) (Number of Tumors Included)		
Study	**Medulloblastoma**	**Ependymoma**	**Pilocytic Astrocytoma**
Schneider et al., (2007)	0.79 ± 0.12 (7)	-	-
Chen et al., (2010)	0.56 ± 0.05 (6)	-	-
Mohamed et al., (2013)	0.72 ± 0.19 (7)	1.13 ± 0.13 (9)	1.53 ± 0.22 (14)
Domínguez-Pinilla et al., (2016)	-	0.9 ± 0.21 (9)	1.29 ± 0.31 (22)
Zitouni et al., (2017)	0.71 ± 0.21 (18)	1.04 ± 0.22 (10)	1.43 ± 0.28 (14)
Novak et al., (2021)	0.87 ± 0.15 (55)	1.13 ± 0.12 (26)	1.66 ± 0.29 (36)
Taheri et al., (2021)	0.87 ± 0.02 (22)	1.20 ± 0.06 (14)	-

Table 3 *– Summary of the reported mean ADC values from the papers included in the meta-analysis.*

	Mean ADC ($mm^2 \times 10^{-3}$)			
Tumor	**N**	**Mean**	**Standard Deviation**	**CoV**
Medulloblastoma	115	0.76	0.16	0.20
Ependymoma	68	1.10	0.10	0.09
Pilocytic Astrocytoma	86	1.49	0.16	0.11

Table 4 *- Summary of reported results for mean ADC of solid tumor tissue in pediatric cohorts of medulloblastoma, ependymoma and pilocytic astrocytoma. The coefficient of variation (CoV) is also calculated as* σ/μ.

Tumors in Calculation	**Optimization for Sensitivity/Specificity**		**Optimization for Weighted Classification Accuracy**		**Optimization for Balanced Classification Accuracy**	
	Mean ADC cut-off values	**Achieved Sensitivity / Specificity**	**Mean ADC cut-off values**	**Achieved Weighted Classification Accuracy**	**Mean ADC cut-off values**	**Achieved Balanced Classification Accuracy**
MB, EP, PA	MB/EP: 0.96 EP/PA: 1.26	MB: 0.90 / 0.98	MB/EP: 0.97 EP/PA: 1.24	MB: 0.95	MB/EP: 0.95 EP/PA: 1.27	MB: 0.89
		EP: 0.89 / 0.91		EP: 0.91		EP: 0.90
		PA: 0.92 / 0.98		PA: 0.96		PA: 0.92

Table 5 *- The cut-off values and achieved performed metrics for mean ADC when all three tumors are considered.*

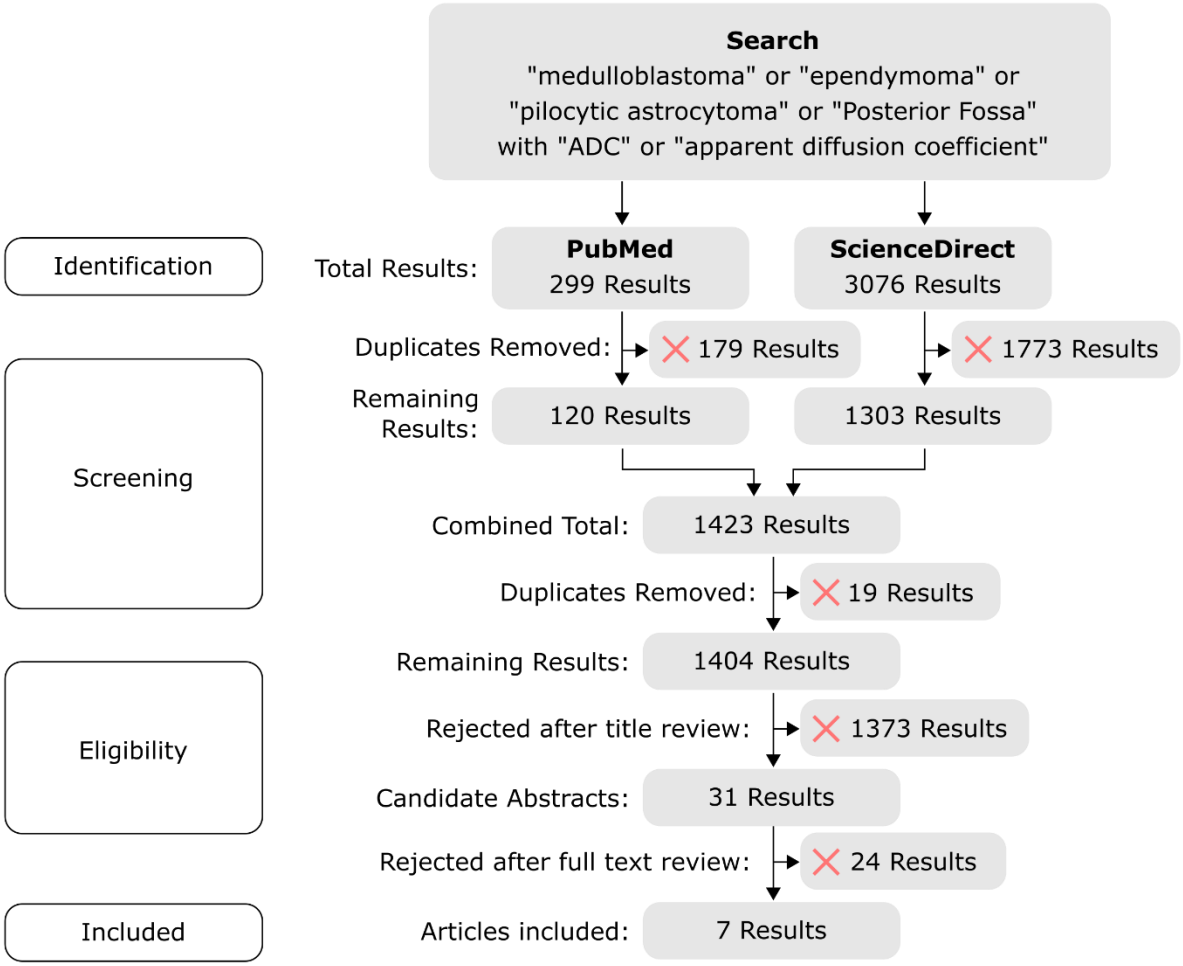

Figure 1 *- Literature search flowchart for identifying relevant papers through PubMed and ScienceDirect.*

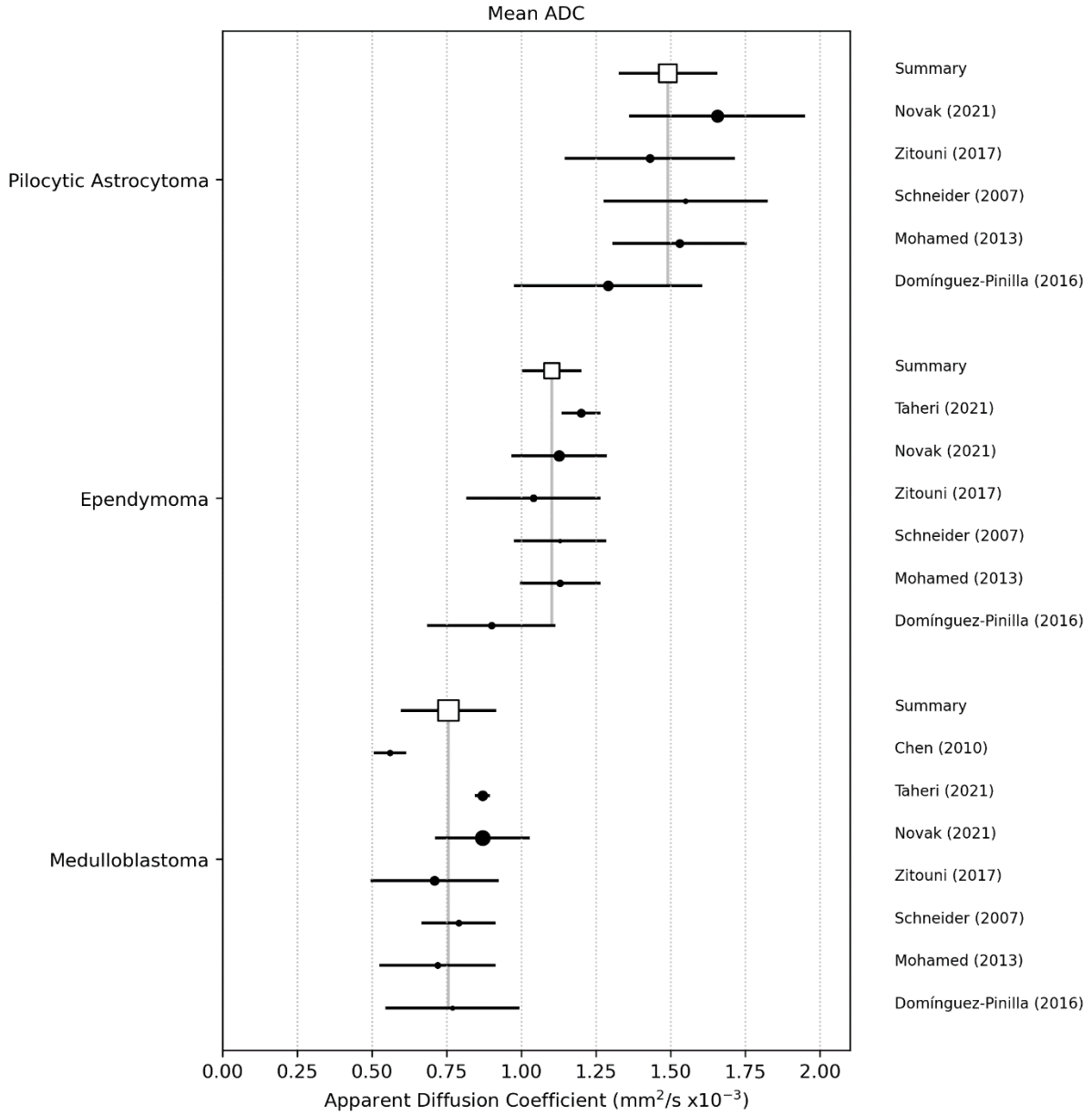

Figure 2 *- Summary of the reported mean ADC values for medulloblastoma, ependymoma and pilocytic astrocytoma. The size of the point represents the number of cases in the study, the bar represents the standard deviation, and the white square is the combined mean and standard deviation.*

- Medulloblastoma ADC
- Ependymoma ADC
- “Pilocytic Astrocytoma” ADC
- Medulloblastoma “Apparent Diffusion Coefficient”
- Ependymoma “Apparent Diffusion Coefficient”
- “Pilocytic Astrocytoma” “Apparent Diffusion Coefficient”

Appendix 1 *– List of terms used in PubMed and ScienceDirect literature searches to find ADC measurements of medulloblastoma, ependymoma and pilocytic astrocytoma.*

	Risk of Bias				**Applicability Concerns**		
Study	**Patient Selection**	**Index Test**	**Reference Standard**	**Flow and Timing**	**Patient Selection**	**Index Test**	**Reference Standard**
Chen (2010)	Low	Low	Low	Low	None	None	None
Domínguez-Pinilla (2016)	Low	Low	Low	Low	None	None	None
Mohamed (2013)	Low	Low	**High**	Low	None	None	**Some**
Novak (2021)	Low	Low	Low	Low	None	None	None
Schneider 2007)	Low	Low	Low	Low	None	None	None
Taheri (2021)	Low	Low	**High**	Low	None	None	**Some**
Zitouni (2017)	Low	Low	Low	Low	None	None	None

Appendix 2 *– The risk of bias for each study was assessed using QUADAS-2 bias assessment tool.*

Tumors in Calculation	**Optimization for Sensitivity/Specificity**		**Optimization for Weighted Classification Accuracy**		**Optimization for Balanced Classification Accuracy**	
	<u>Mean</u> ADC cut-off values	**Achieved Sensitivity / Specificity**	**<u>Mean</u> ADC cut-off values**	**Achieved Weighted Classification Accuracy**	**<u>Mean</u> ADC cut-off values**	**Achieved Balanced Classification Accuracy**
MB, EP	MB/EP: 0.96	MB: 0.91 / 0.93 EP: 0.93 / 0.91	MB/EP: 0.97	MB: 0.97 EP: 0.97	MB/EP: 0.95	MB: 0.89 EP: 0.94
MB, PA	MB/PA: 1.12	MB: 0.99 / 0.99 PA: 0.99 / 0.99	MB/PA: 1.12	MB: 0.99 PA: 0.99	MB/PA: 1.12	MB: 0.99 PA: 0.99
EP, PA	EP/PA: 1.26	EP: 0.95 / 0.93 PA: 0.93 / 0.95	EP/PA: 1.24	EP: 0.94 PA: 0.94	EP/PA: 1.27	EP: 0.96 PA: 0.92

Appendix 3 *– The cut-off values and achieved performed metrics for mean ADC when two tumors are considered.*